Calcitonin receptor-like receptor guides arterial differentiation in zebrafish

Stefania Nicoli,[1] Chiara Tobia,[1] Laura Gualandi,[1] Giulia De Sena,[1] and Marco Presta[1]

[1]Unit of General Pathology and Immunology, Department of Biomedical Sciences and Biotechnology, University of Brescia, Brescia, Italy

The calcitonin receptor-like receptor (*crlr*) is a major endothelial cell receptor for adrenomedullin, a peptide vasodilator involved in cardiovascular development, homeostasis, and disease. Here, we used the zebrafish (*Danio rerio*) model to characterize the role of *crlr* in vascular development. *Crlr* is expressed within somites from the 4- to the 13-somite stage and by arterial progenitors and axial vessels during zebrafish development. Loss of *crlr* results in profound alterations in vascular development and angiogenesis, including atrophic trunk dorsal aorta and interruption of anterior aortic bifurcation, delay in intersomitic vessel development, and lack of blood circulation. Remarkably, *crlr* morphants are characterized by the loss of arterial endothelial cell identity in dorsal aorta, as shown by the lack of expression of the arterial markers *ephrin-B2a*, *DeltaC*, and *notch5*. Down-regulation of *crlr* affects *vascular endothelial growth factor* (*vegf*) expression, whereas *vegf* overexpression is sufficient to rescue arterial differentiation in *crlr* morphants. Finally, genetic and biochemical evidences indicate that somitic *crlr* expression is under the control of *sonic hedgehog*. These data demonstrate that *crlr* plays a nonredundant role in arterial differentiation, representing a novel element of the *sonic hedgehog–vegf-notch* signaling cascade that controls arterial/venous fate. (Blood. 2008;111:4965-4972)

Introduction

The calcitonin receptor-like receptor (*crlr*) is a promiscuous 7-transmembrane G protein–coupled receptor (GPCR) that binds various ligands by forming complexes with different receptor activity-modifying proteins (RAMPs).[1] The interaction of crlr protein with RAMP-2 or RAMP-3 leads to the formation of heterodimeric complexes representing the functional receptors for adrenomedullin, a peptide vasodilator involved in cadiovascular stresses and tumor angiogenesis.[2] *crlr* is highly expressed in endothelium,[3] and *crlr*-null mice die in utero at midgestation with hydrops fetalis and developmental abnormalities in cardiovascular tissues.[4] Remarkably, *adrenomedullin*-null mice show a similar cardiovascular phenotype that provides compelling genetic and in vivo evidence that *crlr* is the primary receptor through which adrenomedullin acts during embryonic development.[4]In vertebrates, the large midline artery and vein are the first blood vessels to develop via a vasculogenic process that involves migration, differentiation, and assembly of the *vascular endothelial growth factor* (*vegf*) *receptor-2* (*kdr*)$^+$ angioblasts from the lateral posterior mesoderm.[5] Molecular differences exist between arterial and venous endothelial cells before the onset of circulation and the activation of complex genetic pathways specifies artery and vein identity, leading to the expression of specific arterial and venous markers (eg, *ephrin-B2a* and *ephB4*, respectively).[6] Genetic alterations of arterial/venous specification are hypothesized to be responsible for congenital hereditary arteriopathies. Indeed, mutations of *notch* pathway components involved in arterial specification are associated with congenital defects of the cardiovascular system.[7]

The zebrafish (*Danio rerio*) has emerged as an useful tool for the genetic analysis of development processes and as a model for human genetic diseases.[8] The optical transparency and ability to survive for 3 to 4 days without functioning circulation make the zebrafish embryo especially amenable for vascular biology studies.[9] Experimental evidences in zebrafish have shown that a signaling pathway controlled by *sonic hedgehog* (*shh*), *vegf*, and *notch* drive arterial/venous cell fate determination.[10] Suppression of *shh* activity leads to *vegf* down-regulation and prevents arterial differentiation that can be rescued by *vegf* overexpression, thus demonstrating that *shh* acts upstream of *vegf*. On the other hand, *vegf* is unable to rescue artery gene marker expression in embryos lacking *notch* function, whereas exogenous *notch* activity can induce arterial differentiation in the absence of *vegf*. Thus, a *shh-vegf-notch* signaling cascade is responsible for inducing arterial differentiation.[11] However, other factors may contribute to the arterial differentiation process (reviewed in Lawson and Weinstein[12]).

Recently, the activation of an adrenomedullin signaling pathway in coordination with *vegf* and *notch* activity has been implicated in the differentiation of arterial endothelial cells from *kdr*$^+$ vascular precursors in murine embryonic stem cell cultures.[13] In the present study, we performed the characterization and functional analysis of the adrenomedullin receptor *crlr* during vascular development in zebrafish. *Crlr* is expressed within the somites in early and midsomitogenesis and in angioblasts and blood vessels of the zebrafish embryo. Embryos lacking *crlr* activity show profound alterations in vascular development and angiogenesis, characterized by arterial malformations, defects in intersomitic vessel (ISV) sprouting and organization, and lack of blood circulation. In association with these morphologic defects, *crlr* knockdown causes the down-regulation of *vegf* and *notch5*

Submitted October 12, 2007; accepted March 5, 2008. Prepublished online as *Blood* First Edition paper, March 7, 2008; DOI 10.1182/blood-2007-10-118166.

The online version of this article contains a data supplement.

The publication costs of this article were defrayed in part by page charge payment. Therefore, and solely to indicate this fact, this article is hereby marked "advertisement" in accordance with 18 USC section 1734.

expression and prevents arterial differentiation. Genetic and biochemical evidences indicate that *crlr* is a *shh*-regulated element that controls arterial differentiation by acting upstream of *vegf*. The results demonstrate for the first time that *crlr* plays a nonredundant role in arterial development.

Methods

Zebrafish stocks

Wild-type AB, transgenic tg(*fli1*:EGFP)^{y1},[11] and *VEGFR2:G-RCFP*[14] zebrafish lines (the latter provided by A. Rubinstein, Zygogen, Atlanta, GA) were maintained as described.[15] Zebrafish embryos were staged as described.[16]

Molecular cloning of zebrafish crlr

A BLAT search[17] on the University of California Santa Cruz Genome Bioinformatics Site (http://genome.ucsc.edu) using the human *crlr* amino acid sequence as a query identifies 2 homolog genes in the zebrafish genome present on chromosome 9 (*crlr-1*; expressed sequence tag [EST] zgc:100872) and chromosome 6 (*crlr-2,* EST LOC567131), respectively. Real-time reverse transcription–polymerase chain reaction (RT-PCR) analysis was performed using the following primer sets: zebrafish *crlr-1* (forward: 5′-AGCTGCTGGACGATTTGTCT-3′, reverse: 5′-TCCAGTGCCTTCTCAAAACC-3′); and zebrafish *crlr-2* (forward: 5′-CACAATCCTCTGCTGCTTCA-3′, reverse 5′- CGCTGTTTTTTGTGATCGT-3′). The PCR fragment with the full-length coding sequence of *crlr-1* was cloned into the TOPO vector (Invitrogen, Carlsbad, CA).

The deduced amino acid sequence of zebrafish *crlr-1* was aligned with *Mus musculus* and *Homo sapiens* crlr protein sequences using the clustaw alignment algorithm of Vector NTI Advance 10.1.1 software (Invitrogen). Structural features of amino acid sequences of zebrafish crlr protein were predicted using ExPASy Proteomics tools (http://ca.expasy.org/tools/).

Whole-mount in situ hybridization

Digoxigenin- and fluorescin-labeled RNA probes were transcribed from linear cDNA constructs (Roche Applied Science, Indianapolis, IN). Whole-mount in situ hybridization (ISH) was performed as described.[18]

Double fluorescence ISH was performed using the TSA Cyanine 3 and 5, TMR, Fluorescein Evaluation Kit (PerkinElmer, Waltham, MA). For sectioning, fixed embryos were dehydrated in an ethanol series, cleared in toluene, and paraffin embedded for 2 hours.

Morpholino-mediated knockdown of *crlr* and chemical treatment

Antisense morpholino (MO) oligonucleotides (Gene Tools, Corvallis, OR) *crlr*-MO1 (5′-AGCTCGCTGTCATCTTCTTTGGCAT-3′) and *crlr*-MO2 (5′-TGTACTAATGTGTTGTGTCTCTACCTC-3′) were directed against the 5′ untranslated region (UTR) spanning the *crlr-1* ATG start codon and the predicted splice donor site at the end of exon 2 of the immature *crlr-1* mRNA, respectively. Std-MO (5′-CCTCTTACCTCAGTTACAATTTATA-3′) was used as a control. Routinely, MOs were microinjected in 4.0 nL volume into 1- to 4-cell stage embryos at the concentration of 0.2 mM for each MO unless specified otherwise. A subset of embryos was coinjected with 0.2 mM of *crlr*-MO1 or std-MO and murine *crlr* mRNA (50 ng μL^{-1}, kindly provided by W. Born, University of Zurich, Switzerland) or $vegf_{121}$ mRNA[11] (2 ng μL^{-1}, kindly provided by N. Lawson, University of Massachusetts, Worcester, MA).

Fertilized eggs were treated in E3 buffer containing DMSO as a vehicle, 50 μM cyclopamine, or 2.5 μg/mL GS4012 (Calbiochem, San Diego, CA) and allowed to develop at 28.5°C.

Microangiography

Tetramethylrhodamine isothiocyanate (TRITC)–dextran (molecular weight 2.0×10^6; Invitrogen) was dissolved in double distilled water at 20 mg/mL and microinjected into the sinus venosus/cardinal vein of zebrafish embryos at 50 hpf as described.[19]

Microscopy

Embryos were mounted in agarose-coated dishes and photographed under an epifluorescence Leica MZ16 F stereomicroscope (1× Plan Apo objective, NA 0.141) equipped with DFC480 digital camera and ICM50 software version 2.8.1 (all from Leica, Wetzlar, Germany). Confocal images were acquired with a Leica TCS SP2 confocal laser microscope (20×/0.7 NA, HC Plan Apo objective), and confocal stacks were assembled using Imaris software version 6.0 (Bitplane, Zurich, Switzerland).

Quantitative RT-PCR analysis

Total RNA was extracted from 40 embryos per group and treated with DNase using the RNeasy Micro kit (Qiagen, Valencia, CA). RT products were amplified in the real-time PCR reaction with Bio-Rad iCycler iQ Real-Time PCR Detection System using an iQ SYBR Green Supermix (Bio-Rad, Hercules, CA) according to the manufacturer's instructions. Primer sequences were as follows: *ephrin-b2a* (forward: 5′-cccatttcccccaaagacta-3′, reverse: 5′-cttccccatgaggagatgc-3′); *flt4* (forward: 5′-actggtcgacttcaacactgg-3′, reverse: 5′-atccaggacgttacgcagag-3′); *β-actin* (forward: 5′-cgtgacatcaaggagaagct-3′, reverse: 5′-tcgtggataccgcaagattc-3′); *vegf* (forward: 5′-tgctcctgcaaattcacacaa-3′, reverse: 5′-atcttggcttttcacatctgcaa-3′); *kdra* (forward: 5′-tggagttccagcacccttta-3′, reverse: 5′-cgtccttcttcacccttttca-3′); and *shh* (forward: 5′-aaagcccacattcattgctc-3′, reverse: 5′-atccaggacgttacgcagag -3′).

Data in triplicate were normalized for zebrafish *β-actin* expression and represent the percentage change in morphant embryos relative to controls. All the experiments were repeated 4 times with similar results.

Results

Molecular cloning and sequence analysis of zebrafish *crlr*

A BLAT search[17] on the UCSC Genome Bioinformatics Site using the human *crlr* amino acid sequence as a query identifies 2 homolog genes in the zebrafish genome present on chromosome 9 (*crlr-1*) and chromosome 6 (*crlr-2*), respectively. Ensembl analysis (zebrafish assembly version 7, Sanger Institute, Cambridge, United Kingdom) of exon-intron organization and syntenic neighboring genomic contest of both genes reveals that zebrafish *crlr-1* represents the homolog of the human *crlr* gene present on chromosome 2. Moreover, RT-PCR expression analysis of both genes at different stages of development (from 0 to 3 dpf) reveals that *crlr-1* is expressed throughout zebrafish development, whereas *crlr-2* is expressed only in maternal stage (Figure S1A, available on the *Blood* website; see the Supplemental Materials link at the top of the online article). On this basis, we focused our study on the expression and function of *crlr-1*, hereafter named *crlr*, during zebrafish development.

The full-length 1.49-kb zebrafish *crlr* transcript (GenBank[20] accession no. NM_001004010) was cloned from the total RNA isolated from zebrafish embryos at 24 hpf. The cDNA encodes for a putative 472–amino acid protein with the characteristic hormone receptor domain and the 7-transmembrane class-B GPCR domain present in *crlr* homologs in other species (Figure S1B). Protein sequence comparison revealed that zebrafish crlr protein is highly homologous to human and murine crlr proteins, with 78% to 79% and 92% to 94% similarity in the hormone receptor and GPCR domains, respectively. Also, cysteine residues essential for a proper adrenomedullin interaction[21] are conserved in the extracellular amino-terminal domain of zebrafish crlr (Figure S1B).

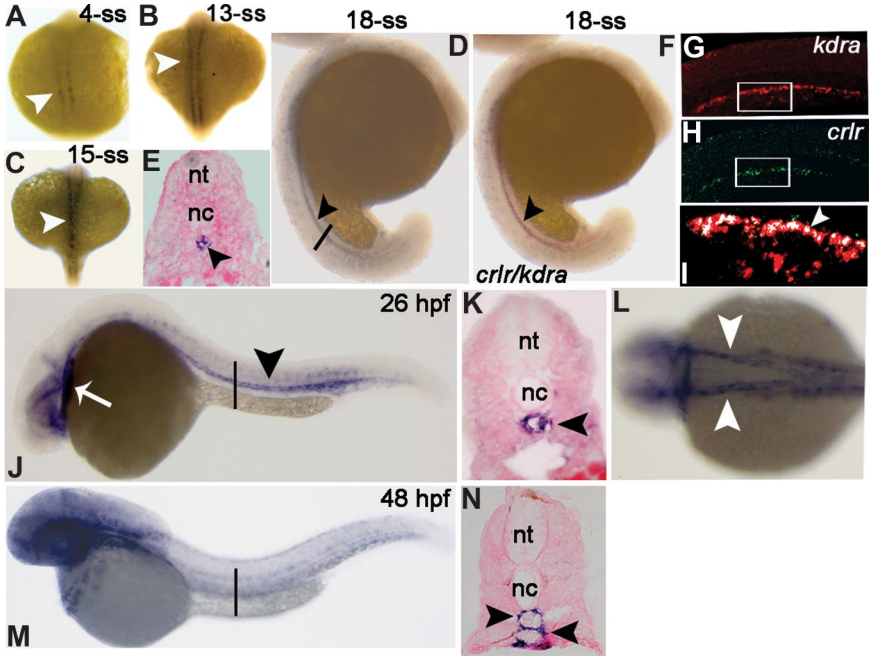

Figure 1. Zebrafish *crlr* is expressed in somites, endothelial cells, and their precursors. *Crlr* expression was analyzed in zebrafish embryos by ISH at the indicated developmental stages. Embryos are anterior to the left and lateral to the top, except in panels A-C and L that represent dorsal views. (E,K,N) The transverse sections through the trunk are highlighted as vertical black bars in panels D, J, and M, respectively. At 4-ss (A) and 13-ss (B) *crlr* is expressed within the somites (white arrowheads). At 15-ss, white arrowhead points to *crlr* expression along a midline through the trunk (C). At 18-ss (D,E) *crlr* is expressed in the midline under the notochord (black arrowhead). At this stage, double ISH (F) shows the expression of *crlr* (blue) by *kdra*$^+$ angioblasts (red). Confocal laser microscopy shows a detail of the tail region of 18-ss embryo after double fluorescence ISH for *kdra* (red in panel G) and *crlr* (green in panel H); the area in white boxes are merged in panel I, where white arrowheads point to the layer of *crlr*$^+$/*kdra*$^+$ DA angioblasts close to the notochord (merged signal in white). (J) At 26 hpf, *crlr* is expressed by blood vessels of the head, in the heart tube (white arrow), and in DA of the trunk (black arrowhead). (K) Cross-section of a 26-hpf embryo, confirming *crlr* expression in DA (black arrowhead). At this stage, *crlr* is expressed also by the right- and left-lateral DA (panel L; white arrowheads). At 48 hpf, lateral view (M) and cross-section (N, black arrowheads) demonstrate *crlr* expression in both DA and PCV.

Temporal and spatial expression pattern of *crlr*

We analyzed the expression pattern of the *crlr* gene in early zebrafish embryos by whole-mount ISH. No expression was observed prior to the 1-somite stage (1-ss; S.N., unpublished observations, February 2007). From the 4-ss, *crlr* is expressed within the medial aspect of the newly formed somites immediately adjacent to the notochord (Figure 1A). Somite expression is maintained until the 13-ss (Figure 1B), being lost thereafter. At the 15- to 18-ss, a stripe of *crlr*$^+$ cells is apparent in the midline and extends through the trunk and posterior part of the embryo (Figure 1C,D), likely representing the endothelial precursor cells migrated to the future axial vascolature region under the nothocord (Figure 1E). To assess this hypothesis, *crlr* expression was analyzed by double ISH with the early endothelial marker vegf receptor-1 *kdra*, mainly expressed in dorsal aorta (DA) progenitor cells.[22] At 18-ss, *crlr* stains in the same field of *kdra*$^+$ endothelial cells proximal to the notochord (Figure 1F). Confocal laser double fluorescence ISH with *kdra* (Figure 1G) and *crlr* (Figure 1H) probes confirmed that the most dorsal *kdra*$^+$ DA angioblasts coexpress *crlr* (Figure 1I).

At 26 hpf, *crlr* expression is maintained in the axial vasculature of the trunk (Figure 1J); cross-sections at this level showed that *crlr* marks the main medial DA (Figure 1K). Also, *crlr* is expressed in the right- and left-lateral DA (Figure 1L) and rostrally in the primitive internal carotid arteries (Figure 1J). We also observed *crlr* expression in heart tube at this stage (Figure 1J). At 48 hpf, *crlr* is expressed both in the DA and in the posterior cardinal vein (PCV) of the trunk (Figure 1M,N), and it is widely expressed in the vasculature of the head and in the pectoral fin mesoderm (S.N., unpublished observations, February 2007).

MO knockdown of *crlr* function results in vascular defects

To assess the functional role of *crlr* in zebrafish vascular development we used an antisense MO knockdown approach.[23] To this purpose, a MO was designed directed against the 5′ UTR spanning the *crlr* ATG start codon to inhibit protein translation (*crlr*-MO1). tg(*fli1*:EGFP)^{y1} transgenic zebrafish embryos in which EGFP expression is driven by the promoter of the panendothelial marker *fli-1* were injected at the 1- to 4-cell stage with 0.8 pmol/embryo of *crlr*-MO1 or of control std-MO, and the development of GFP-labeled blood vessels was directly observed in live embryos.

Whole-mount microscopic analysis of 28-hpf *crlr* morphants revealed no obvious morphological abnormalities, with *crlr*-MO1–injected embryos appearing slightly thinner than control embryos (Figure 2A,B). However, *crlr* morphants showed defects in vascular morphology and circulatory patterns. Indeed, *crlr*-MO1–injected embryos showed no apparent blood circulation and displayed a disorganized trunk vessel plexus with a remarkable reduction in the size of DA (Figure 2D). At variance, embryos injected with control MO exhibited normal blood circulation and vasculature morphology, as indicated by fully lumenized well-defined trunk vessels (Figure 2C).

Confocal laser microscopy confirmed the presence of a disorganized trunk vessel plexus and of poorly defined boundaries between the DA and PVC in tg(*fli1*:EGFP)^{y1} embryos injected with *crlr*-MO1 when compared with embryos injected with std-MO (Figure 2F,H). Moreover, *crlr* knockdown caused a delay in ISV development (Figure 2H). Indeed, only a few ISV sprouts were detectable in *crlr* morphants at 28 hpf, whereas std-MO–injected embryos showed normally developed ISVs that, sprouted bilaterally from the DA, have migrated dorsally between the somites,

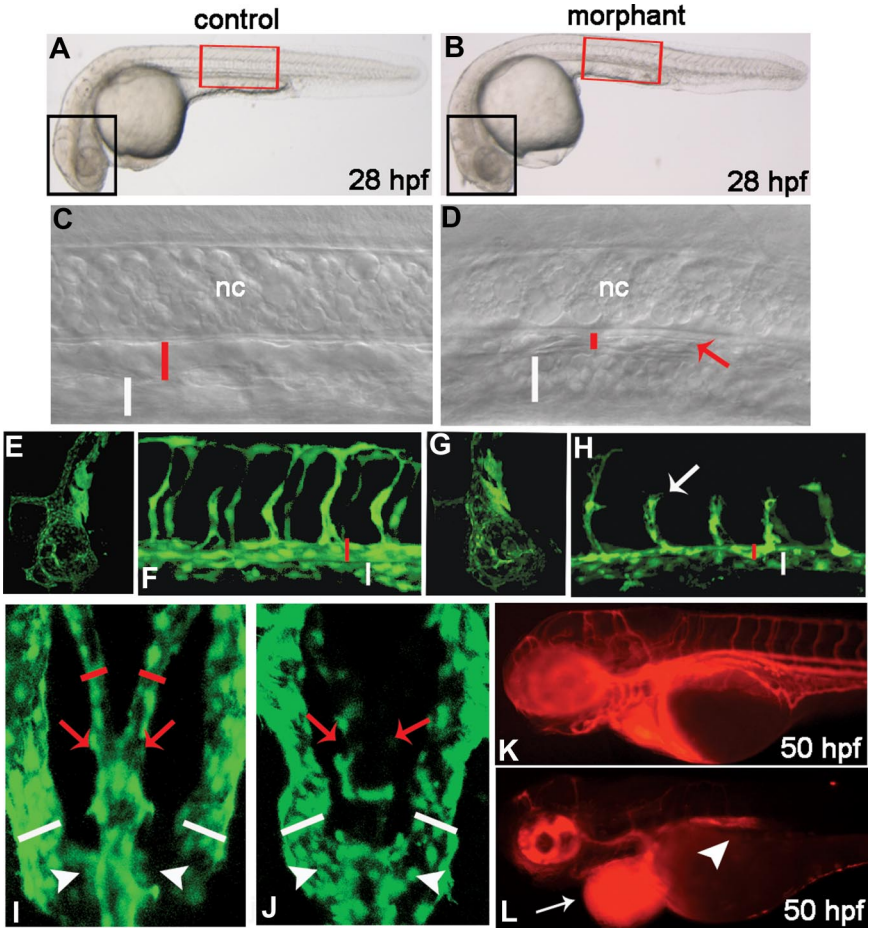

Figure 2. Crlr knockdown results in vascular defects. Vascular morphology in tg(*fli1*:EGFP)^{y1} embryos injected with std-MO (control in panels A,C,E,F,I, and K) or *crlr*-MO1 (morphant in panels B,D,G,H,J, and L). Morphologic appearance of control (A) and *crlr* morphant (B) embryos at 28 hpf (head and trunk regions are highlighted by black and red boxes, respectively). Differential interference contrast images of the trunk region (lateral view) of live zebrafish embryos injected with std-MO (C) or *crlr*-MO1 (D), the lumen of DA and PCV are indicated by red and white bars, respectively; note the abnormal size of DA and the presence of cells with endothelial morphology (red arrow) in proximity to the notochord in *crlr* morphant (D). Confocal laser microscopy showing details of the head (E,G) and trunk (F,H) regions (lateral view) in std-MO– and *crlr*-MO1–injected tg(*fli1*:EGFP)^{y1} embryos (DA [red bar], PVC [white bar]; white arrow points to poorly developed ISVs in *crlr* morphant). *Crlr* knockdown causes also an interruption of the vascular tube at the bifurcation of the DA. Dorsal view of the lateral dorsal aortae (red arrows) and of cardinal vein branches (white arroweads) in control (I) and *crlr*-MO1–injected (L) tg(*fli1*:EGFP)^{y1} embryos; lumens of the lateral dorsal aortae and cardinal vein branches are indicated by red and white bars, respectively. Note the poor lumenization and formation of lateral aortae branches in *crlr* morphant compared with the posterior cardinal vein. Microangiography performed at 50 hpf shows that blood circulation is confined to the head and heart regions (white arrow) in *crlr* morphants (L) when compared with control embryos (K). White arrowhead in panel L points to the interruption of the blood flow at the level of bifurcation of the DA.

assuming a typical T shape (Figure 2F). As development continues, ISVs do not follow the normal stereotypical intersomitic pathway in *crlr* morphants (S.N., unpublished observations, March 2007). Moreover, dorsal view of *crlr*-MO1–injected tg(*fli1*:EGFP)^{y1} embryos showed that lateral dorsal aortae are thin and fail to lumenize, with an evident interruption at the level of the anterior aortic bifurcation (Figure 2J) when compared with the lumenized lateral dorsal aortae of control embryos (Figure 2I). In contrast, PCV branches are similar in control and *crlr* morphants (Figure 2I,J). Microangiography was performed at 50 hpf to further assess the impact of aortic dysmorphogenesis on the integrity of the circulation in *crlr*-MO1–injected embryos. *Crlr* morphants were characterized by the lack of blood circulation that was occasionally limited to the circulation of the trunk as a consequence by the blockade of the blood flow at the level of the anterior aortic bifurcation (Figure 2K,L). Also, blood pooling was observed in the cardiac region (Figure 2L). At variance with the observed alterations in the trunk vasculature, 28-hpf *crlr* morphants showed no evident alterations in the vasculature of the head when compared with control embryos (Figure 2E,G). The vascular defects observed in *crlr*-MO1–injected embryos are summarized in Table 1.

To better characterize the defects in the developing vasculature, *crlr* morphants were analyzed for *fli-1* expression by ISH. At 8-ss, the expression of panendothelial *fli-1*, together with that of notochord *no-tail*[24] and of nascent somite *myoD*,[25] were not affected in *crlr* morphants, thus indicating the lack of alterations in the vascular and nonvascular differentiation programs prior to this time of development (Figure S2). In keeping with the data obtained with tg(*fli1*:EGFP)^{y1} embryos, the *fli-1* transcript was abundantly expressed in the axial vasculature of both control and *crlr* morphants at 28 hpf, indicating that endothelial cell migration and localization is not defective in the embryos lacking *crlr* activity. However, also in this case, a reduction in the angiogenic development of *fli-1*$^{+}$ ISVs was observed in *crlr* morphants when compared with controls (Figure S2).

Table 1. Summary of the vascular defects in *crlr* morphant embryos

Lack of blood circulation	Alterations in ISV development	Alterations in trunk DA development	Interruption at the anterior DA bifurcation	*crlr*-MO1, % of injected embryos± SD	*crlr*-MO2, % of injected embryos± SD
–	–	–	–	14 ± 2	35 ± 7
+	–	+	–	21 ± 6	21 ± 4
+	–	+	+	20 ± 4	26 ± 10
+	+	+	+	45 ± 4	9 ± 1

One- to 4-cell stage zebrafish *VEGFR2:G-RCFP* embryos were injected with 0.8 pmol *crlr*-MO1 (n = 34) or *crlr*-MO2 (n = 25), and vascular defects were assessed at 28 hpf. Data are expressed as percentage of morphants showing the indicated vascular defect(s). The results are the mean plus or minus SD of two independent experiments. No vascular defects were observed in std-MO–injected embryos (n = 32). – indicates absence of the phenotypic defect; +, presence of the phenotypic defect.

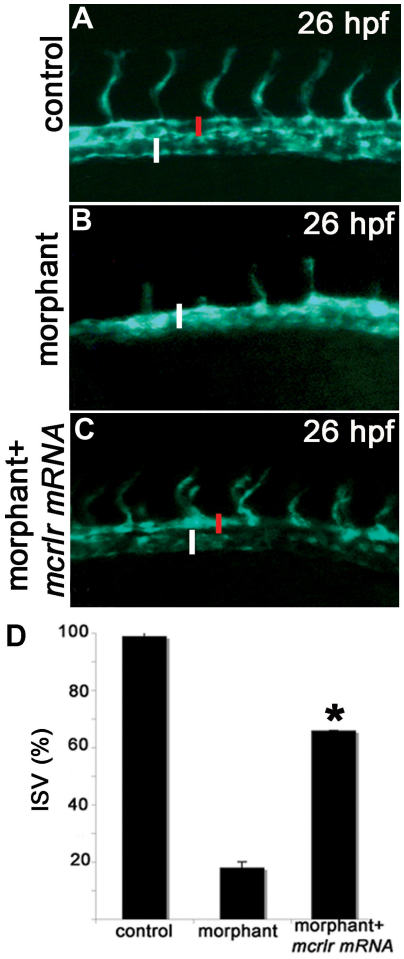

Figure 3. Murine *crlr* overexpression rescues the vascular phenotype in zebrafish *crlr* morphants. Murine *crlr* mRNA was injected in *VEGFR2:G-RCFP crlr* morphants, and axial vasculature of the trunk was examined under an epifluorescence microscope at 26 hpf. The reduction in size of DA (red bar) and the delay in ISV development observed in *crlr* morphants (B) are rescued by murine *crlr* overexpression (C). (A) control *VEGFR2:G-RCFP* embryo. PCV is indicated by the white bar. The percentage of embryos showing normal ISV development in the different experimental groups is shown in panel D. Data are the mean plus or minus SD of 2 independent experiments with 15 embryos per group. *Statistically different from the "morphant" group; $P < .02$, Student *t* test.

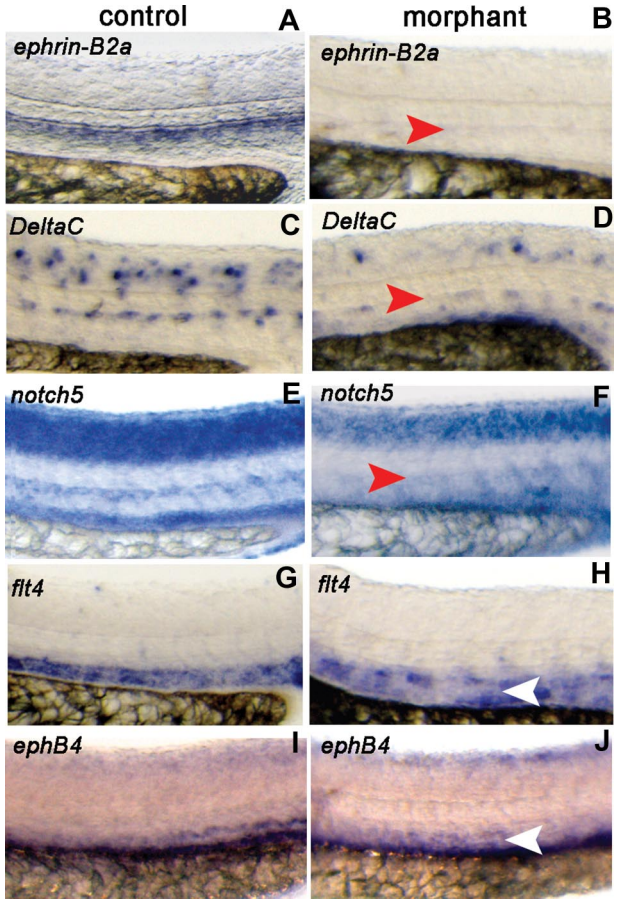

Figure 4. Crlr knockdown affects arterial gene expression. Std-MO–injected embryos (control) and *crlr*-MO1–injected embryos (morphant) were analyzed at 26 hpf for the expression of the indicated arterial and venous markers by ISH. Lateral view of the trunk region is shown (DA, red arrowheads; PCV, white arrowheads). *Crlr* morphants were characterized by lack of expression of *ephrin-B2a* (panel B; 13 of 17 embryos examined), *DeltaC* (panel D; 13 of 19 embryos examined), and *notch5* (panel F; 10 of 13 embryos examined). In contrast, venous markers *flt4* (H) and *ephB4* (J) were expressed in 7 of 10 and in 11 of 12 *crlr* morphants, respectively. Arterial and venous markers were instead expressed in all the control embryos examined (ranging between 10 and 16 embryos per gene investigated).

To confirm the specificity of the vascular defects in *crlr* morphants, *crlr*-MO1 was coinjected with a MO-resistant form of the murine *crlr* mRNA. In 2 independent experiments, analysis of the embryos at 28 hpf showed the ability of the murine transcript to rescue the *crlr*-knockdown phenotype as assessed by the presence of normally developed ISVs in 66% of rescued embryos (10 of 15 embryos in both experiments) compared with 16% of *crlr* morphants (2 of 15 embryos and 3 out of 15 embryos in the 2 experiments, respectively; $P < .02$, Student *t* test; Figure 3).

To further confirm that the phenotype observed in *crlr*-MO1–injected embryos is specifically related with *crlr* knockdown, embryos were injected with a different *crlr*-specific MO targeted against the splice donor site at the end of exon 2 of the immature *crlr* mRNA (*crlr*-MO2). Injection of *crlr*-MO2 caused vascular defects similar to those caused by *crlr*-MO1 even though with a lower frequency (Table 1) due to the noncomplete blockade of *crlr* mRNA maturation (S.N., unpublished observations, May 2007).

Taken together, these findings indicate a nonredundant vascular function for *crlr* in vivo. In particular, *crlr* appears to play a major role in aortic vessel development.

Arterial endothelial markers are lost in *crlr* morphants

To assess whether *crlr* plays a specific role in arterial differentiation during vascular development in zebrafish, we examined the expression of arterial- and venous-specific markers[11] in axial vessels of the trunk in std-MO– and *crlr*-MO1–injected embryos at 26 hpf. When compared with std-MO–injected embryos, *clrl* morphants show a specific loss of the expression of the arterial genes *ephrin-B2a*, *DeltaC*, and *notch5* in the DA (Figure 4A-F), whereas their expression in other districts of the embryo was not significantly affected (Figure S3A). To determine the effects on venous cell fate, we assayed for expression of *flt4* which is initially expressed in both arterial and venous primordial cells and becomes restricted to venous vessels by 24 hpf.[26] Embryos injected with std-MO and *crlr*-MO1 showed the typical down-regulation of *flt4* in the DA and its normal expression in PCV (Figure 4G,H). Also, the expression of the venous marker *ephB4* was not affected in the PCV of *crlr*-MO1–injected embryos (Figure 4I,J). In keeping

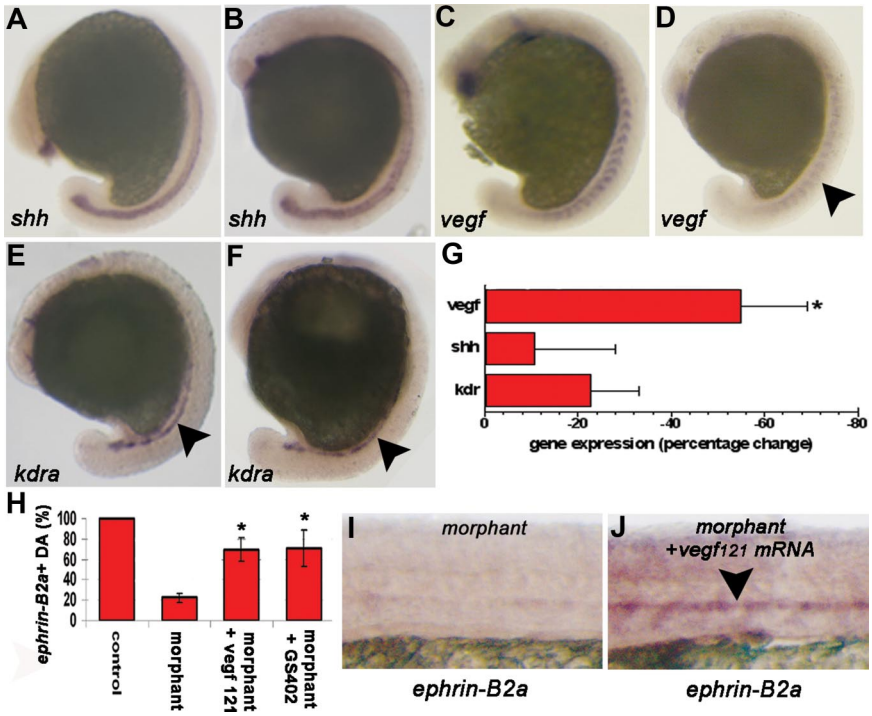

Figure 5. Crlr acts upstream of vegf in modulating arterial differentiation in zebrafish. Std-MO–injected embryos (A,C,E) and *crlr*-MO1–injected embryos (B,D,F) were analyzed at 15-ss for *shh*, *vegf*, and *kdra* expression by ISH (panels A-F; embryos are anterior to the left and lateral to the top). No changes in *shh* notochord expression (panel B; n = 15) and in endothelial progenitor *kdra* expression (panel F; n = 13) were observed in *crlr* morphants when compared with controls (A,E). Note the proper expression and localization of the *kdra* staining in *crlr* morphant embryos (black arrowhead in panel F) when compared with control embryos (black arrowhead in panel E). In contrast, somitic *vegf* expression was reduced in 20 of 32 morphants examined (panel D; black arrowhead). No changes in gene expression were instead observed in control std-MO–injected embryos when compared with uninjected embryos (n = 25, data not shown). (G) Total RNA was extracted at 15-ss from 40 embryos per group, and *shh*, *vegf*, and *kdra* expression were evaluated by real-time RT-PCR. Data in triplicate were normalized for zebrafish β-*actin* expression and represent the percentage change in morphant embryos relative to controls. Similar results were obtained in 4 independent experiments (*$P < .05$ vs controls; Student *t* test). (H) *ephrin-B2a* expression was assessed at 26 hpf in the DA of the trunk of *GFP* mRNA–injected control embryos (n = 30), *crlr* morphants (n = 25), $vegf_{121}$ mRNA–injected *crlr* morphants (n = 25), and GS402-treated *crlr* morphants (n = 25) and data were expressed as percentage of positive embryos. The results are the mean plus or minus SD of 3 independent experiments (*$P < .05$ vs crlr morphants, Student *t* test). (I,J) representative images of the trunk of *crlr* morphant (I) and $vegf_{121}$ mRNA-injected *crlr* morphant (J) embryos showing the ability of *vegf* overexpression to rescue *ephrin-B2a* expression in the DA of *crlr* morphants (black arrowhead).

with these observations, real-time RT-PCR analysis showed a significant decrease of *ephrin-B2a* expression, but not of *flt4* expression, in *crlr* morphants when compared with control embryos (Figure S3B).

Consistent with the morphologic vascular defects, these data demonstrate that *crlr* has a function in zebrafish arterial differentiation and development.

Crlr genetically interacts with the *vegf* pathway during arterial differentiation

Angioblasts within the zebrafish lateral mesoderm are restricted to arterial or venous fate during mid-somitogenesis.[10,27] At this stage, *shh* in the notochord modulates the somitic expression of *vegf* which, in turn, regulates the arterial differentiation of the first *flk-1*$^+$ angioblasts migrating toward the midline.[11,28] As shown, *crlr* is also expressed within the somites at this stage, suggesting that impaired arterial differentiation in zebrafish embryo lacking *crlr* activity might be the consequence of defects in the *shh*/*vegf* genetic pathway.

To assess this hypothesis, we investigated the expression of *shh*, *vegf*, and *kdra* in 15-ss embryos injected with *crlr*-MO1 or std-MO. Whole-mount ISH and real time RT-PCR analysis of *crlr* morphants shows a significant and reproducible down-regulation of *vegf* expression within the somites, with no significant changes in *shh* expression in the notochord (Figure 5A-G). Also, *kdra*$^+$ angioblasts migrating toward the midline were normally present at this time of development in *crlr* morphants when compared with control embryos (Figure 5E,F). The concomitant down-regulation of *ephrin-B2a* and *vegf* activity in embryos lacking *crlr* raises the possibility that *vegf* may provide a signal for arterial differentiation downstream of *crlr*. On this basis, to assess whether exogenous *vegf* is sufficient to rescue *ephrin-B2a* expression in the absence of *crlr* activity, *crlr* morphants were injected with the mRNA encoding for zebrafish $vegf_{121}$ and assayed for the expression of *ephrin-B2a* at 26 hpf. As shown in Figure 5H-J, the injection of 5 pg/embryo of $vegf_{121}$ mRNA rescued the expression of *ephrin-B2a* in DA, whereas no *ephrin-B2a* stain was detectable in the trunk of *crlr* morphants injected with control *GFP* mRNA. A similar rescue was observed also after treatment of *crlr*-MO1–injected embryos with GS4012, a potent *vegf* inducer[29] (Figure 5H). These results indicate that *vegf* overexpression is sufficient to rescue arterial differentiation in the absence of *crlr* activity and suggest that the loss of *ephrin-B2a* expression in *crlr* morphants is due to the down-regulation of *vegf* activity downstream of *crlr*.

Shh provides a signal upstream of *vegf* to modulate arterial differentiation.[11] On this basis, we investigated *crlr* transcript levels in embryos lacking *shh* activity. Embryos carrying a null mutation for *sonic-you* (syu^{t4} mutants) and wild-type embryos treated with 25 μM cyclopamine, a potent inhibitor of *shh* signaling,[30] fail to express somitic *crlr* at 10-ss (Figure S4). These results demonstrate that *shh* modulates *crlr* somite expression in a putative *shh*/*crlr*/*vegf* pathway. In keeping with

this hypothesis, *shh* overexpression fails to induce *vegf* up-regulation and causes only a limited *ephrin-B2a* expression in *crlr* morphants when compared with *shh*-overexpressing control embryos (Figure S5).

Discussion

In this study, we report the characterization and functional analysis of *crlr*, a major adrenomedullin receptor, in zebrafish. Previous studies in murine models have implicated the adrenomedullin/crlr system in cardiovascular development, homeostasis, and disease.[31] Here we show that *crlr* has a nonredundant function in zebrafish arterial differentiation and development.

In zebrafish, *crlr* is expressed in early and mid-somitogenesis within the medial aspect of the newly formed somites immediately adjacent to the notochord. Then, *crlr* is expressed in *kdra*$^+$ angioblasts that will coalesce into the presumptive DA. At later stages, *crlr* is expressed by the endothelium of the head and of axial vasculature, first in DA (at 26 hpf) and then also in PCV (at 48 hpf). Consistent with this expression pattern, knockdown of *crlr* activity by specific MOs results in profound effects on the vasculature of the zebrafish embryo, characterized by delay and alterations in ISV development, dysmorphogenesis of DA of the trunk and interruption at the level of the anterior aortic bifurcation, and lack of blood circulation. Defects in aortic bifurcation have been observed also in embryos lacking *vegf* or *phospolipase C gamma-1* activity[32] and in *gridlock* zebrafish mutants.[33] However, similar to that observed in *notch* mutants,[22] suppression of *crlr* function in zebrafish does not affect *gridlock* expression (S.N., unpublished observations, May 2007). Interestingly, only minor, if any, defects in the vasculature of the head were observed in *crlr* morphants, suggesting that *crlr* function is redundant for head vascularization or that the remaining amount of crlr protein activity may be sufficient for normal head vessel development.

The vascular defects in the trunk of *crlr* morphants are associated with an impairment of aortic endothelial cell differentiation, as shown by the lack of expression of the specific arterial markers *ephrin-B2a*, *DeltaC*, and *notch5*. Despite the loss of artery-specific gene expression, the DA is present in its proper location, which indicates a defect in the differentiation of aortic endothelial cells, rather than a defect of angioblasts to migrate and form this vessel structure. Indeed, *kdra* expression is normal at 10-ss (S.N., unpublished observations, April 2007), and *kdra*$^+$ angioblasts are properly located under the notochord at 15-ss, indicating that the formation and migration of DA progenitors are *crlr* independent. Moreover, the expression patterns of the panendothelial marker *fli-1* and of the *kdr* promoter-driven GFP are not affected by suppression of *crlr* activity. Finally, the effect of *crlr* knockdown appears to be limited to artery specification, with no effect being observed by *crlr*-MO injection on the expression of the venous genes *flt4* and *ephB4* in PCV.

Arterial differentiation in zebrafish is under the control of a *shh-vegf-notch* pathway.[11] Our data indicate that *crlr* affects this pathway by modulating *vegf* activity. Indeed, suppression of *crlr* function causes a significant, even though not complete inhibition of somitic *vegf* expression, with no effects on *shh* expression. This is in keeping with the *vegf* down-regulation observed in mice knocked out for the crlr ligand adrenomedullin.[34] *vegf* MO experiments have shown that the penetrance of the vascular phenotypes associated with the lack of *vegf* activity is strictly dose dependent.[35] Accordingly, the vascular defects observed in *crlr* morphants, including alterations in ISV development and DA maturation, resemble the least severe phenotypic alterations detectable in zebrafish embryos injected with low doses of *vegf* MO and in heterozygous *vegfa* mutant mice.[36] In keeping with these observations, *vegf* overexpression is sufficient to rescue arterial differentiation in *crlr* morphants.

Shh plays a key role in arterial differentiation by acting upstream of vegf.[11] Here, we show that also *crlr* is a *shh*-modulated gene in zebrafish. Indeed, inhibition of *shh* function, as it occurs in syu^{t4} mutants or in cyclopamine-treated embryos, results in a complete down-regulation of somitic *crlr* expression. Also, in keeping with a putative *shh/crlr/vegf* pathway, *shh* overexpression fails to induce *vegf* up-regulation in *crlr* morphants. However, *crlr* overexpression does not rescue *vegf* signaling and arterial differentiation in cyclopamine-treated embryos and in syu^{t4} mutants lacking *shh* activity (S.N., unpublished observations, June 2007 and January 2008), indicating that *crlr* is necessary but not sufficient to drive arterial differentiation.

Although our observations indicate that somitic *crlr* modulates *vegf* expression to regulate arterial differentiation, we cannot rule out a direct role for endothelial *crlr* in DA formation and angiogenesis at later stages of development, as also suggested by its expression in specified DA progenitors as well as in the endothelium of axial vessels. Indeed, *crlr* morphants show a significant delay in ISV development. Relevant to this point is the observation that alterations of vascular homeostasis, including arteriosclerosis and tumor angiogenesis, are associated with alterations in the adrenomedullin/receptor system.[2] Accordingly, *crlr* down-regulation following *crlr*-MO1 injection strongly inhibits tumor angiogenesis when zebrafish embryos are grafted with proangiogenic mammalian tumor cells[37,38] (Figure S6). Finally, it is interesting to note that the homolog of the human adrenomedullin receptor (*admr*), a gene encoding for a protein distinct from crlr, has been shown to be expressed in the endothelium of developing zebrafish.[39] Even though the biological function of this receptor has not been elucidated, it will be of importance to establish its relationship, if any, with *crlr* in mediating the biological activity of adrenomedullin during development and vascular pathologies.

In vitro observations had shown that adrenomedullin signaling acts synergistically with *vegf* to induce in vitro arterial differentiation in murine embryonic stem cell cultures.[13] Here, we demonstrate that the major adrenomedullin receptor *crlr* is a novel element of the genetic cascade that controls arterial differentiation in vivo.

Acknowledgments

The authors wish to thank F. Cotelli (University of Milan) for helpful discussion and criticisms, S. Mitola (University of Brescia) for her advice in fluorescence microscopy, and N. Lawson (University of Massachusetts) for the vegf expression vector and criticisms.

This work was supported by grants from Istituto Superiore di Sanità (Oncotechnological Program), Ministero dell'Istruzione, Università e Ricerca (Centro di Eccellenza per l'Innovazione Diagnostica e Terapeutica, Cofin projects), Associazione Italiana per la Ricerca sul Cancro, Fondazione Berlucchi, and NOBEL Project Cariplo to M.P.

Authorship

Contribution: S.N. and M.P. designed research; S.N., C.T., L.G., and G.S. performed research; S.N. and M.P. analyzed the data; and S.N. and M.P. wrote the paper.

Conflict-of-interest disclosure: The authors declare no competing financial interests.

Correspondence: Marco Presta, General Pathology, Department of Biomedical Sciences and Biotechnology, University of Brescia, Viale Europa 11, 25123 Brescia, Italy; e-mail: presta@med.unibs.it.

References

1. McLatchie LM, Fraser NJ, Main MJ, et al. RAMPs regulate the transport and ligand specificity of the calcitonin-receptor-like receptor. Nature. 1998; 393:333-339.
2. Ribatti D, Nico B, Spinazzi R, Vacca A, Nussdorfer GG. The role of adrenomedullin in angiogenesis. Peptides. 2005;26:1670-1675.
3. Hagner S, Stahl U, Knoblauch B, McGregor GP, Lang RE. Calcitonin receptor-like receptor: identification and distribution in human peripheral tissues. Cell Tissue Res. 2002;310:41-50.
4. Caron KM, Smithies O. Extreme hydrops fetalis and cardiovascular abnormalities in mice lacking a functional Adrenomedullin gene. Proc Natl Acad Sci U S A. 2001;98:615-619.
5. Risau W. Differentiation of endothelium. FASEB J. 1995;9:926-933.
6. Adams RH, Wilkinson GA, Weiss C, et al. Roles of ephrinB ligands and EphB receptors in cardiovascular development: demarcation of arterial/venous domains, vascular morphogenesis, and sprouting angiogenesis. Genes Dev. 1999;13: 295-306.
7. Niessen K, Karsan A. Notch signaling in the developing cardiovascular system. Am J Physiol Cell Physiol. 2007;293:C1-C11.
8. Lieschke GJ, Currie PD. Animal models of human disease: zebrafish swim into view. Nat Rev Genet. 2007;8:353-367.
9. Weinstein B. Vascular cell biology in vivo: a new piscine paradigm? Trends Cell Biol. 2002;12:439-445.
10. Torres-Vazquez J, Kamei M, Weinstein BM. Molecular distinction between arteries and veins. Cell Tissue Res. 2003;314:43-59.
11. Lawson ND, Vogel AM, Weinstein BM. sonic hedgehog and vascular endothelial growth factor act upstream of the Notch pathway during arterial endothelial differentiation. Dev Cell. 2002;3:127-136.
12. Lawson ND, Weinstein BM. Arteries and veins: making a difference with zebrafish. Nat Rev Genet. 2002;3:674-682.
13. Yurugi-Kobayashi T, Itoh H, Schroeder T, et al. Adrenomedullin/cyclic AMP pathway induces Notch activation and differentiation of arterial endothelial cells from vascular progenitors. Arterioscler Thromb Vasc Biol. 2006;26:1977-1984.
14. Cross LM, Cook MA, Lin S, Chen JN, Rubinstein AL. Rapid analysis of angiogenesis drugs in a live fluorescent zebrafish assay. Arterioscler Thromb Vasc Biol. 2003;23:911-912.
15. Westerfield M. The Zebrafish book. Eugene, OR: University of Oregon Press; 1995.
16. Kimmel CB, Ballard WW, Kimmel SR, Ullmann B, Schilling TF. Stages of embryonic development of the zebrafish. Dev Dyn. 1995;203:253-310.
17. Kent WJ. BLAT—the BLAST-like alignment tool. Genome Res. 2002;12:656-664.
18. Paffett-Lugassy NN, Zon LI. Analysis of hematopoietic development in the zebrafish. Methods Mol Med. 2005;105:171-198.
19. Isogai S, Horiguchi M, Weinstein BM. The vascular anatomy of the developing zebrafish: an atlas of embryonic and early larval development. Dev Biol. 2001;230:278-301.
20. National Center for Biotechnology Information. GenBank database. Available: http://www.ncbi.nlm.nih.gov/Genbank/. Accessed April 1, 2008.
21. Kuwasako K, Kitamura K, Uemura T, Nagoshi Y, Kato J, Eto T. The function of extracellular cysteines in the human adrenomedullin receptor. Hypertens Res. 2003;26:S25-S31.
22. Lawson ND, Scheer N, Pham VN, et al. Notch signaling is required for arterial-venous differentiation during embryonic vascular development. Development. 2001;128:3675-3683.
23. Nasevicius A, Ekker SC. Effective targeted gene "knockdown" in zebrafish. Nat Genet. 2000;26: 216-220.
24. Kawahara A, Che YS, Hanaoka R, Takeda H, Dawid IB. Zebrafish GADD45beta genes are involved in somite segmentation. Proc Natl Acad Sci U S A. 2005;102:361-366.
25. Lin CY, Yung RF, Lee HC, Chen WT, Chen YH, Tsai HJ. Myogenic regulatory factors Myf5 and Myod function distinctly during craniofacial myogenesis of zebrafish. Dev Biol. 2006;299:594-608.
26. Thompson MA, Ransom DG, Pratt SJ, et al. The cloche and spadetail genes differentially affect hematopoiesis and vasculogenesis. Dev Biol. 1998;197:248-269.
27. Zhong TP, Childs S, Leu JP, Fishman MC. Gridlock signalling pathway fashions the first embryonic artery. Nature. 2001;414:216-220.
28. Jin SW, Beis D, Mitchell T, Chen JN, Stainier DY. Cellular and molecular analyses of vascular tube and lumen formation in zebrafish. Development. 2005;132:5199-5209.
29. Peterson RT, Shaw SY, Peterson TA, et al. Chemical suppression of a genetic mutation in a zebrafish model of aortic coarctation. Nat Biotechnol. 2004;22:595-599.
30. Cooper MK, Porter JA, Young KE, Beachy PA. Teratogen-mediated inhibition of target tissue response to Shh signaling. Science. 1998;280: 1603-1607.
31. Kato J, Tsuruda T, Kita T, Kitamura K, Eto T. Adrenomedullin: a protective factor for blood vessels. Arterioscler Thromb Vasc Biol. 2005;25: 2480-2487.
32. Lawson ND, Mugford JW, Diamond BA, Weinstein BM. phospholipase C gamma-1 is required downstream of vascular endothelial growth factor during arterial development. Genes Dev. 2003; 17:1346-1351.
33. Weinstein BM, Stemple DL, Driever W, Fishman MC. Gridlock, a localized heritable vascular patterning defect in the zebrafish. Nat Med. 1995;1: 1143-1147.
34. Iimuro S, Shindo T, Moriyama N, et al. Angiogenic effects of adrenomedullin in ischemia and tumor growth. Circ Res. 2004;95:415-423.
35. Nasevicius A, Larson J, Ekker SC. Distinct requirements for zebrafish angiogenesis revealed by a VEGF-A morphant. Yeast. 2000;17:294-301.
36. Ferrara N, Carver-Moore K, Chen H, et al. Heterozygous embryonic lethality induced by targeted inactivation of the VEGF gene. Nature. 1996;380:439-442.
37. Nicoli S, Presta M. The zebrafish/tumor xenograft angiogenesis assay. Nat Protoc. 2007;2:2918-2923.
38. Nicoli S, Ribatti D, Cotelli F, Presta M. Mammalian tumor xenografts induce neovascularization in zebrafish embryos. Cancer Res. 2007;67: 2927-2931.
39. Sumanas S, Jorniak T, Lin S. Identification of novel vascular endothelial-specific genes by the microarray analysis of the zebrafish cloche mutants. Blood. 2005;106:534-541.